

Supporting information

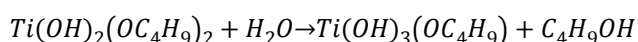
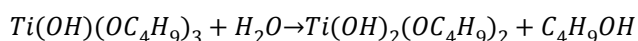
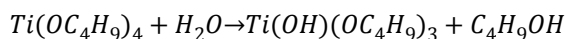
Enhancing Photocatalytic Activity of Disorder-Engineered C/TiO₂ and TiO₂ Nanoparticles

Shu Wang, Lei Zhao, Lina Bai, Junmin Yan, Qing Jiang, Jianshe Lian*

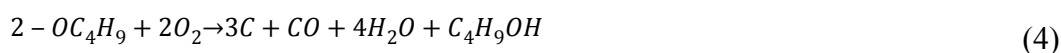
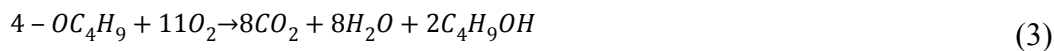
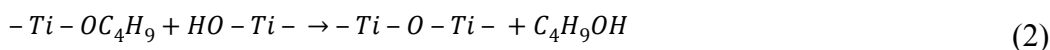
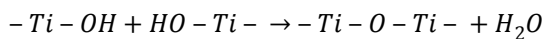
Key Lab of Automobile Materials, Ministry of Education, College of Materials Science and Engineering, Jilin University, Nanling Campus, Changchun, 130025, P.R. China

S1. Sample Preparation:

In a typical sol-gel process, it included the hydrolysis of Ti precursor (Eq.1) and the polycondensation of the products of hydrolysis (Eq.2). During the calcination process, the alkoxy (-OC₄H₉) was oxidized above 350°C under air atmosphere (Eq.3). However, -OC₄H₉ could be carbonized under oxygen-lack atmosphere (Eq.4). Consequently, we proposed a simple and green method to abandon additional carbon sources to synthesize C-TiO₂ hybrid. In our work, we controlled the flow rate of nitrogen at 0.5 L/min to produce a proper oxygen-lack environment to realize the carbonization reaction.



* Corresponding author. E-mail: liansj@jlu.edu.cn
Tel: 86-431-85095876 Fax: 86-431-85095876



S2. Sample Characterizations:

X-ray diffraction (XRD):

The crystal structures of the samples were analyzed by X-ray diffraction (XRD, Rigaku D/MAX 2500PC) with a Cu target and a mono-chromometer at 40 kV and 250 mA. The scanning range was from 20° to 80°. The crystal size from the XRD pattern was calculated using the Scherrer formula, $D = 0.9\lambda / \beta \cos\theta$, where D is the crystal size, λ is the wavelength of the X-ray radiation (0.15418 nm for Cu K $_{\alpha}$ radiation), β is the full width at half maximum (FWHM), and θ is the diffraction angle.

Raman analysis: The multiphonon resonant Raman spectrum was collected using a micro-Raman spectrometer (Renishaw) with a laser of 532 nm wavelength.

High-resolution transmission electron microscopy (HRTEM):

Transmission electron microscopy (TEM) with GIF Quantum was employed to observe the microstructure and electron energy loss spectrum (EELS) of TiO₂ nanocrystalline.

UV-vis analysis:

The optical absorption spectra of samples were obtained at room temperature by the UV-Vis spectrometer equipped with an integrating sphere.

X-Ray Photoelectron spectroscopy (XPS):

XPS with an ESCALAB Mk II (Vacuum Generators) spectrometer was used to detect

complementary information on the chemical combination states of various elements of TiO₂ samples. Cycles of XPS measurements were done in a high-vacuum chamber with a base pressure of 10⁻⁸ Torr. The XPS spectrum was fitted with the nonlinear least-squares fit program using Gauss-Lorentzian peak shapes.

S3. Photocatalytic Experiments

The photocatalytic activities of the samples were characterized by degrading 10 mg/L phenol solution under the simulated solar-driven derived from a 300 W Xenon lamp with an AM 1.5 filter in air at ambient temperature. 10 mg sample was used to degrade 30 ml phenol solution with dilute sulphuric acid titrating to PH 4 through the photo-degradation process. Concentration change of phenol was monitored by the change of the 270 nm absorption peak.

The photocatalytic activities of synthesized catalysts were also evaluated by the degradation of 20 mg/L MB solution, through the change in optical absorption of MB solution at ~664 nm. 10 mg catalyst was used to degrade 30 mL MB solution under the same solar-driven irradiation in an experiment.

Photocatalytic H₂ production was tested in a closed-gas circulation system. 0.6 wt% Pt was loaded as a cocatalyst by UV irradiation of PtCl₄ solution. In a typical experiment, 20 mg of sample was suspended in 30 mL with 1:1 water-methanol solution (containing 0.2 mg PtCl₄) under magnetic stirring. And then the mixture was irradiated by Xe lamp (300 W) for 30 minutes, which enabled the Pt nanoparticles to load on the surface of TiO₂ as cocatalyst. After degassing this system, the photocatalytic water-splitting process was executed under the irradiation of simulated solar-driven light (300 W Xe lamp with an AM 1.5 filter). The H₂ release was analyzed by gas chromatography.

S4. Supporting Figures:

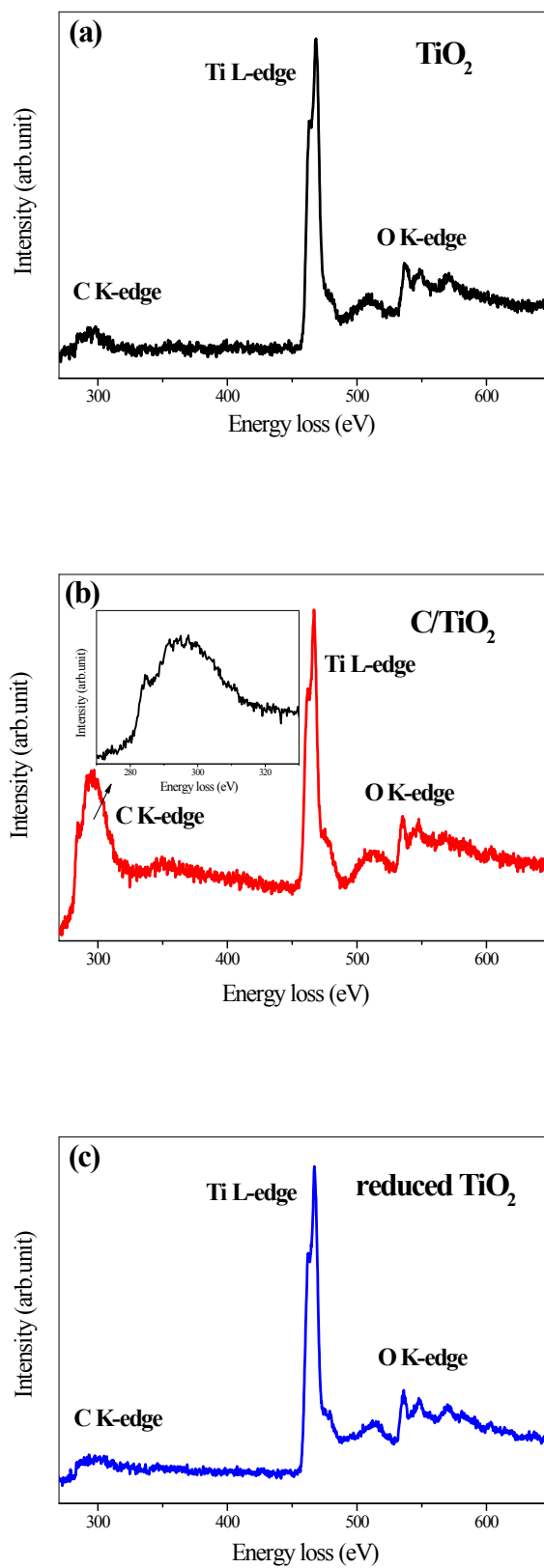
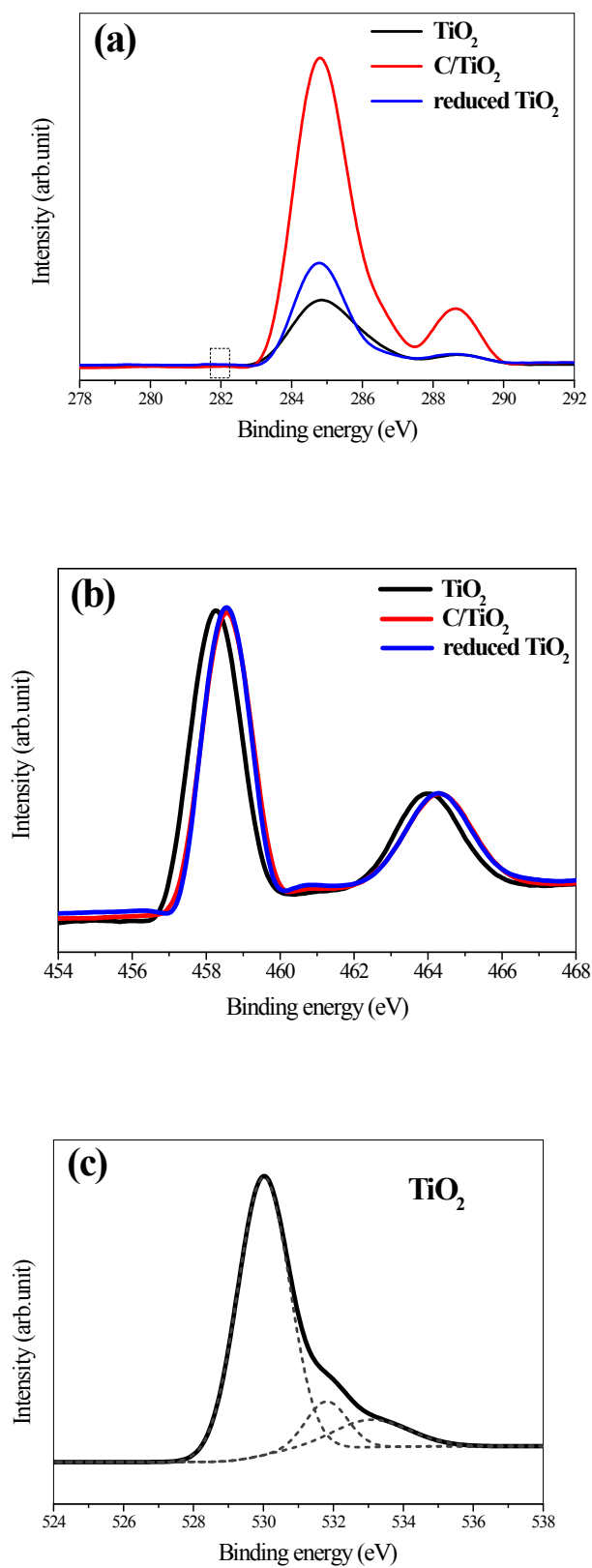


Fig. S1 (a)-(c) EELS spectrum of reference TiO_2 , C/TiO_2 and reduced TiO_2 NPs, respectively. The inset of Figure S1(b) exhibits the EELS spectrum for C K-edge ELNES of C/TiO_2 in detail, which proves the carbon shell exists as

amorphous carbon by its ELNES fingerprints [S1].



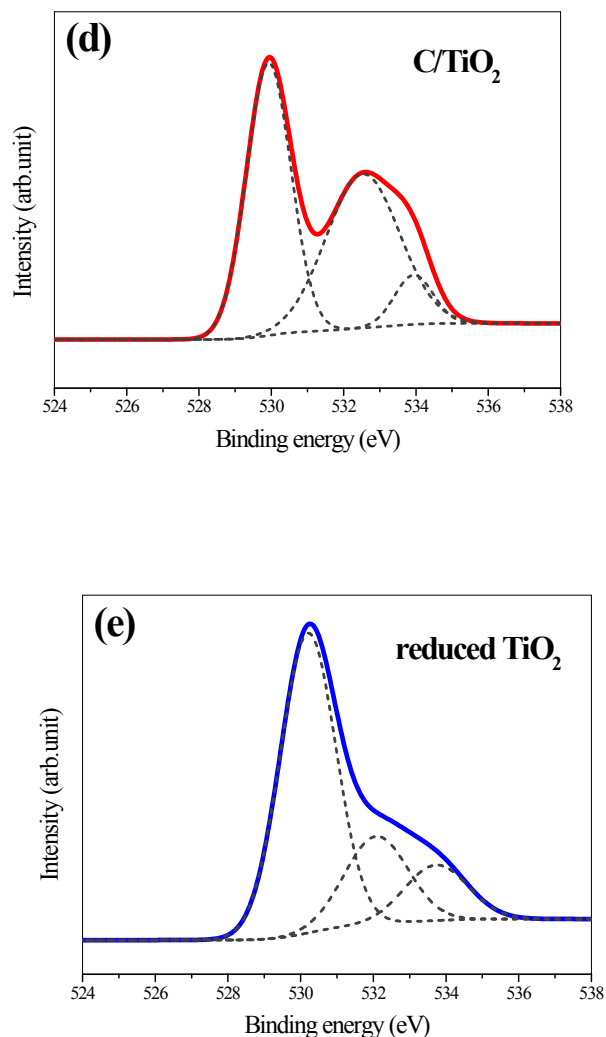


Fig. S2 (a) XP C 1s spectra of reference TiO₂, C/TiO₂ and reduced TiO₂ NPs, respectively. To compare with the experimentally introduced carbon, the strong signal of XP C 1s at 284.8 eV proves the presence of carbon shell in C/TiO₂ NPs, and there is no signal of Ti-C bonding occurred at ~282 eV [28]. **(b)** XP Ti 2p spectra of reference TiO₂, C/TiO₂ and reduced TiO₂ NPs, respectively. In the Ti 2p spectral region, the peaks located at 458.3 vs. 458.6 eV and 464.0 vs. 464.3 eV can be attributed to Ti 2p_{3/2} and Ti 2p_{1/2}, respectively. **(c-e)** XP O 1s spectra of reference TiO₂, C/TiO₂ and reduced TiO₂ NPs, respectively. The Gaussian decomposition procedure reveals that the spectra are mainly composed by three peaks centered at 530.1±0.1 eV, 532.2±0.3 eV and 533.7±0.3 eV, which represent lattice O, adsorbed O₂/V_{OS} and adsorbed H₂O/OH groups, respectively.

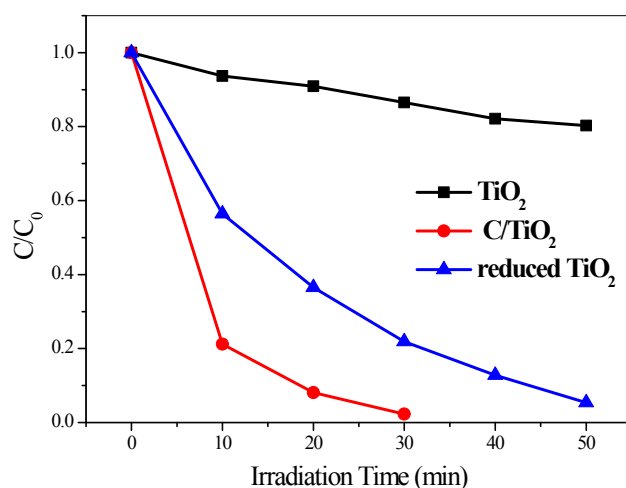


Fig. S3 The photocatalytic activity of the reference TiO₂, C/TiO₂ and reduced TiO₂ NPs for the decomposition of methyl blue, respectively.

S5. Supporting Table:

Table S1 Refined structural parameters, lattice strain and optical bandgap of samples calculated by XRD and absorption spectra.

	reference	C/TiO ₂	reduced TiO ₂
	TiO ₂		
a (Å)	3.78534	3.78692	3.78374
b (Å)	3.78534	3.78692	3.78374
c (Å)	9.51609	9.48	9.49485
V (Å ³)	136.35	135.95	135.93
2θ (°) & FWHM	25.34 & 0.383	25.24 & 0.782	25.22 & 0.602
Lattice strain	0.004336	0.01294	0.008796
Optical bandgap (eV)	3.3	2.9	3.2

Reference:

[S1] F. Hofer and P. Golob, Ultramicroscopy, 1987, **21**, 379-383.